

DamageArbiter: A CLIP-Enhanced Multimodal Arbitration Framework for Hurricane Damage Assessment from Street-View Imagery

Yifan Yang^a, Lei Zou^{a*}, Wenjing Gong^b, Kani Fu^c, Zongrong Li^a, Siqin Wang^d, Bing Zhou^e, Heng Cai^a, Hao Tian^a

^aDepartment of Geography, Texas A&M University, College Station, USA

^bDepartment of Landscape Architecture & Urban Planning, Texas A&M University, College Station, USA

^cDepartment of Industrial and Systems Engineering, University of Florida, Gainesville, USA

^dSpatial Sciences Institute, University of Southern California, Los Angeles, USA

^eDepartment of Geography and Sustainability, University of Tennessee, Knoxville, USA

*Corresponding author: lzou@tamu.edu

Abstract

Analyzing street-view imagery with computer vision models for rapid, hyperlocal damage assessment is becoming popular and valuable in emergency response and recovery, but traditional models often act like “black boxes”, lacking interpretability and reliability. This study proposes a multimodal disagreement-driven Arbitration framework powered by Contrastive Language-Image Pre-training (CLIP) models, DamageArbiter, to improve the accuracy, interpretability, and robustness of damage estimation from street-view imagery. DamageArbiter leverages the complementary strengths of unimodal and multimodal models, employing a lightweight logistic regression meta-classifier to arbitrate cases of disagreement. Using 2,556 post-disaster street-view images, paired with both manually generated and large language model (LLM)-generated text descriptions, we systematically compared the performance of unimodal models (including image-only and text-only models), multimodal CLIP-based models, and DamageArbiter. Notably, DamageArbiter improved the accuracy from 74.33% (ViT-B/32, image-only) to 82.79%, surpassing the 80% accuracy threshold and achieving an absolute improvement of 8.46% compared to the strongest baseline model. Beyond improvements in overall accuracy, compared to visual models relying solely on images, DamageArbiter, through arbitration of discrepancies between unimodal and multimodal predictions, mitigates common overconfidence errors in visual models, especially in situations where disaster visual cues are ambiguous or subject to interference, reducing overconfidence but incorrect predictions. We further mapped and analyzed geo-referenced predictions and misclassifications to compare model performance across locations. Overall, this work advances street-view-based disaster assessment from coarse severity classification toward a more reliable and interpretable framework.

Keywords: Contrastive Language-Image Pre-training (CLIP), Disaster Assessment, Street-View Imagery, Disagreement-driven arbitration, Multimodal Learning

1. Introduction

Timely and accurate post-disaster damage assessments play a pivotal role in supporting emergency response, guiding resource allocation, and informing short-term and long-term recovery efforts. Among the diverse data sources employed in disaster assessment, street-view imagery has emerged as a valuable source for ground-level assessments of disaster impacts, offering high-resolution, human perspectives of structural and infrastructural damages that are often challenging to capture from aerial or satellite imagery (Lozano & Tien, 2023; Yamazaki & Matsuoka, 2007; Ye et al., 2024).

Traditional approaches to street-view-based damage assessments typically rely on pre-trained computer vision models fine-tuned on manually labeled datasets (H. Li et al., 2024; Xue et al., 2024; Zhai & Peng, 2020). Architectures such as Visual Geometry Group network (VGG), the Shifted Window Transformer (Swin Transformer), and ConvNeXt have been applied to classify disaster damage based on street-view images, but several critical limitations exist. First, they rely on extensive manual annotations, which are costly and time-consuming to adapt quickly to new or evolving disaster scenarios. Second, even when large, annotated datasets are available, the labels are often limited to coarse categories, typically three or four damage levels, providing limited insights into the underlying causes. For example, an image labeled as “severe” may reflect the destruction of a large building, the collapse of critical infrastructure (e.g., power poles), or both. Third, interpreting results from these models remains difficult. Previous work has leveraged tools such as Gradient-weighted Class Activation Mapping (Grad-CAM) to explain how vision models interpret disaster damages from images (Selvaraju et al., 2017; Yang et al., 2025). Grad-CAM identifies spatial regions within an image that contribute most strongly to a model’s prediction, but it lacks the capacity to convey fine-grained semantic information such as the specific damage type, severity, and its implications, which are essential for actionable decision-making.

Recent advances in vision-language models (VLMs) open promising new avenues for disaster assessment with data like street-view imagery. By aligning images with descriptions, VLMs can capture richer semantics from images to support fine-grained reasoning and generate interpretable outputs. In particular, the Contrastive Language-Image Pretraining (CLIP) model provides a general framework for cross-modal alignment that can be adapted for disaster scenarios. For instance, Yang and Zou (2025) demonstrated the potential of VLMs in perceiving multidimensional disaster damage directly from street-view images. However, the application of VLMs in disaster damage assessment is still in its early stage, primarily due to the lack of high-quality disaster-related datasets of image/text pairs for fine-tuning and benchmarking VLM models (Jayati et al., 2024; Wang et al., 2024). Consequently, there is a critical need for research that shifts focus from sole reliance on accuracy to scrutinize model reliability, interpretability, and practical utility in street-view-based damage assessments.

This research proposes DamageArbiter, a disagreement-driven, CLIP-enhanced multimodal arbitration framework for damage assessment from street-view imagery. The overarching objective is to develop and benchmark this framework against baseline unimodal models (text-only or image-only), specifically evaluating improvements in accuracy, reliability (particularly in mitigating overconfidence), and explainability. A total of 2,556 post-disaster street-view images collected after the 2024 Hurricane Milton, along with textual descriptions generated by human annotators and large language models (LLMs), were used for fine-tuning and performance assessment. We validate the model’s effectiveness and deploy the optimal configuration to geographically visualize spatial patterns of damage types and severities. A key

novelty lies in the disagreement-driven arbitration mechanism, which dynamically resolves conflicts between visual and textual evidence to handle ambiguity in damage assessments. This contributes a methodological advancement by shifting from black-box prediction to a transparent, trust-aware system suitable for high-stakes disaster response.

2. Related Work

2.1 Street-View Imagery and Computer Vision for Disaster Damage Assessment

Street-view imagery has become an increasingly valuable data source for post-disaster damage assessment due to its ability to capture fine-grained, human-level perspectives of damaged buildings, roadways, and infrastructures. Platforms such as Mapillary, Google Street View, and OpenStreetMap (OSM) enable widespread access to such data at different locations and timestamps, facilitating large-scale, hyperlocal, and longitudinal analysis of urban exposure, damage, and resilience to disasters at unprecedented scales (Alvarez Leon & Quinn, 2019; Mahabir et al., 2020; Sánchez & Labib, 2024).

The advancement of deep learning-based computer vision has significantly accelerated research in visual-based disaster analysis and related domains. From a technical perspective, rather than training models from scratch, researchers have adopted fine-tuning strategies using pre-trained visual backbones, leading to notable gains in both classification accuracy and computational efficiency (Gupta, 2021; Ding et al., 2023; Xin et al., 2024). Pre-trained architectures such as Visual Geometry Group network (VGG), Swin Transformer, and ConvNeXt have been widely used in disaster damage classification tasks (Mahabir et al., 2020; Xue et al., 2024; Zhao, Lu, et al., 2024). Swin Transformer leverages hierarchical attention mechanisms to capture both local and global visual patterns (Liu et al., 2021, 2022), while ConvNeXt employs large-kernel convolutions to enhance representational capacity beyond traditional convolutional neural networks (CNNs) (Feng et al., 2022; Woo et al., 2023).

With the growing availability of street-view imagery and the increasing maturity of computer vision models, recent studies have begun to extend these techniques to support disaster-related tasks. For example, Gao et al. (2024) employed a YOLOv5-based computer vision framework to estimate First-Floor Elevation (FFE) from street-view images, providing a scalable alternative to manual field surveys and supporting flood mitigation planning in coastal regions. In parallel, Wang et al. (2024) applied street-view imagery to vulnerability assessment by adopting a Mask Region-based CNN (Mask R-CNN) approach to extract visual features related to building structure, condition, and surrounding infrastructure, and using these indicators as proxies to estimate household-level vulnerability to natural hazards. Overall, these studies demonstrate that the integration of street-view data with deep learning techniques enables computer vision to play an increasingly important role in disaster risk assessment across both natural and built environments.

2.2 Analysis of Street-View Imagery with Vision-Language Models (VLMs)

With the continued scaling of model parameters, vision-language models such as GPT-4o have demonstrated remarkable proficiency in cross-modal understanding, including text generation, vision-language alignment, and multimodal reasoning (OpenAI et al., 2024). These models have been

applied across a wide array of fields, including medicine, biology, education, environmental science, and geographic information science, showcasing their capacity to support complex decision-making (Agathokleous et al., 2023; Gimpel et al., 2023; Q. Wu et al., 2024; Xu et al., 2025; Yang et al., 2024). The integration spans diverse data types such as text, raster, and vector. It positions vision–language models and generative artificial intelligence (GAI) models in roles such as purifier, converter, generator, and reasoner. This convergence marks a shift toward multimodal foundation models that enhance GeoAI's effectiveness, with implications for cross-scale research, autonomous geospatial systems, and intelligent disaster management (Wang et al., 2024).

Vision-Language Models are a class of multimodal models designed to jointly learn representations from visual and textual data, enabling cross-modal understanding and reasoning between images and language. By aligning semantic information across modalities, VLMs have shown strong performance in tasks such as image–text matching, retrieval, and multimodal classification. Among Vision-Language Models, the CLIP model has gained prominence due to its ability to learn aligned representations between textual and visual data (Radford et al., 2021). Geospatial research has adopted CLIP-inspired techniques for tasks such as geo-localization within urban environments, image retrieval, and disaster scene classification by fine-tuning on remote sensing, street-view, or social media imagery (Haas et al., 2023; L. Li et al., 2024; H. Li et al., 2024). The contrastive learning paradigm in CLIP enables effective cross-modal semantic alignment, making it a compelling foundation for disaster-related assessment tasks. For instance, Jayati et al. (2024) integrated ChatGPT-generated textual descriptions with building-based images using CLIP, demonstrating that this multimodal approach outperformed image-only and text-only models in classifying post-hurricane damage levels. Li et al. (2025) developed CLIP-BCA-Gated, which enhances CLIP with cross-attention and adaptive gating to improve text-image alignment, achieving superior performance in real-time disaster crisis classification.

Within the disaster domain, recent studies have begun to explore the use of VLMs for extracting and reasoning about disaster-related content from both textual and visual inputs. GPT-based models have demonstrated the ability to infer geographic locations from street-view imagery, raising critical questions around privacy while highlighting the power of embedded world knowledge in VLMs (Yang et al., 2024; Y. Liu et al., 2024). Similarly, VLMs have exhibited strong zero-shot geolocation capabilities, even in the absence of explicitly labeled geographic datasets (Z. Wang et al., 2024). Beyond geolocation, VLMs have also been applied to disaster assessment, such as generating structured textual descriptions and conducting fine-grained evaluations of disaster impacts. For example, Ma et al. (2025) proposed a multimodal, multilingual pipeline that applies VLMs to fuse text–image social media data for fine-grained earthquake damage assessment, showing strong correlation with seismic intensity data but sensitivity to language, modality, and prompt design.

However, most CLIP-based approaches place limited emphasis on the systematic evaluation of model reliability. Specifically, it remains unclear whether CLIP-based models are prone to overconfident erroneous predictions in complex post-disaster scenarios, i.e., whether the model's overconfidence judgments are actually driven by significant visual or semantic cues unrelated to the disaster itself. On the other hand, when visual and semantic information is insufficient or conflicting, CLIP-based models may also exhibit ambiguity errors, making it difficult for the model to form consistent and stable judgments. Furthermore, the study by Jayati et al. (2024) showed that the classification capabilities of CLIP-based models were not significantly better than those of purely visual models. In addition, many CLIP-related

studies bypass manually annotated text descriptions in practical applications, relying primarily on automatically generated text as semantic input. While this approach reduces data annotation costs to some extent, it may also weaken the model's reliability in disaster assessment tasks and limit its fine-grained understanding of disaster-related semantic details.

Despite these encouraging advances, few studies have systematically examined the ability of visual language models to perform fine-grained disaster damage assessment from post-disaster street view imagery. Specifically, tasks such as identifying disaster-related entities, assessing the severity of disasters, and generating descriptive narratives of post-disaster conditions still require further research. We thereby evaluate the performance of visual language models for disaster assessment by generating coherent, human-agreeable scene descriptions. Together, these contributions highlight the potential of VLMs to enhance automation, reduce annotation burdens, and improve the scalability and interpretability of post-disaster assessment systems.

3. Methodology

The methodological framework consists of four core parts (Figure 1), which gradually promote the expansion of disaster assessment tasks from single-modal feature extraction to multimodal alignment and disagreement-driven arbitration, and then to semantic-level interpretation and systematic performance evaluation.

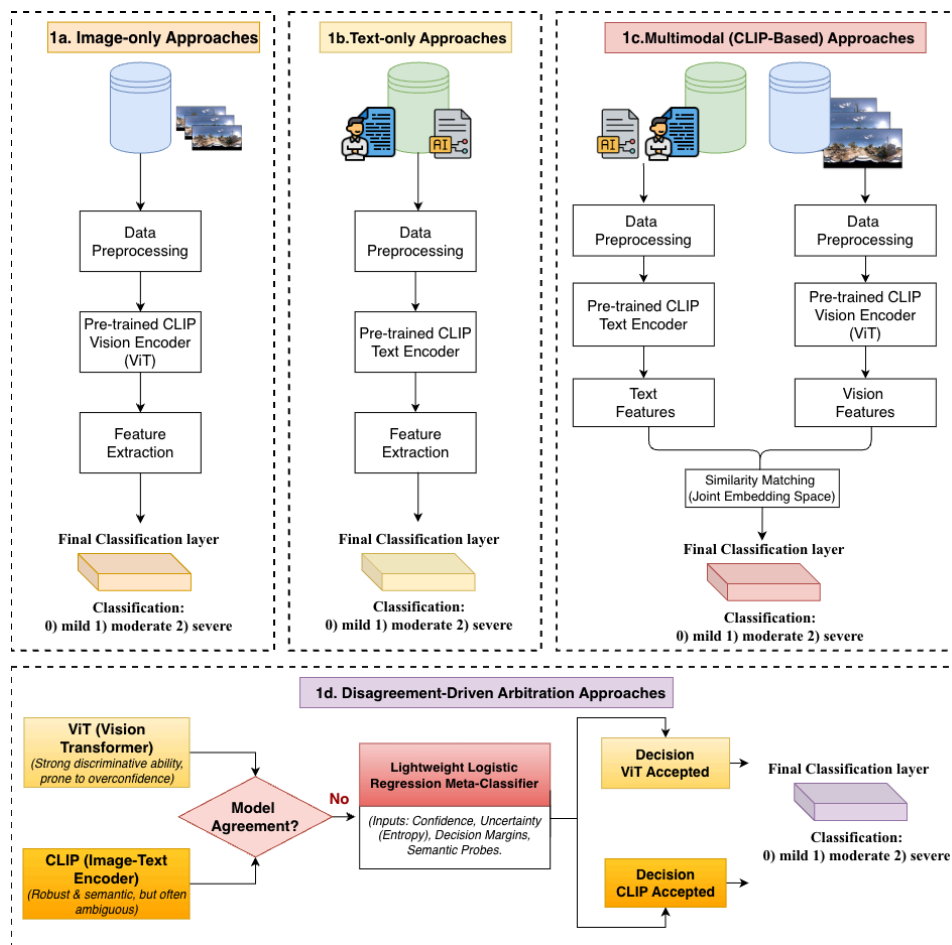


Figure 1. Overall Framework of Disaster Assessment Approaches.

First, in terms of model architecture design (Section 3.1), we developed three approaches: image unimodality (Figure 1a), text unimodality (Figure 1b), and multimodality (Figure 1c), to systematically compare the performance of different input modalities in disaster assessment. Second, to overcome the performance and stability limitations of different architectures, we proposed a disagreement-driven arbitration framework (Figure 1d; detailed in Section 3.2). When ViT and CLIP agree on the prediction, the output is directly generated. In the event of disagreement, a lightweight logistic regression meta-classifier is introduced for arbitration.

3.1 Model Architectures

3.1.1 Vision Transformer (ViT) Architectures

In terms of model architecture, we adopt the Vision Transformer (ViT) as the core baseline for unimodal image processing. We choose ViT over convolutional neural networks for two main reasons. First, as a Transformer-based architecture, ViT is designed to model global contextual relationships in images, which is particularly suitable for disaster scenes characterized by spatially distributed and heterogeneous visual patterns. This design choice is further examined through the experimental results presented in this study. Second, the visual encoder of CLIP is built upon ViT. Using ViT as the unimodal baseline ensures architectural consistency in the experimental design.

Specifically, we used the ViT-Base-Patch16-224 and ViT-Base-Patch32-224 architectures with pre-trained weights from the timm library (Wightman, 2019). As shown in Figure 2, all street view images were uniformly scaled to a 224×224 resolution and normalized during input. Data augmentation operations such as random horizontal flipping were also applied during training to improve model generalization. Subsequently, the images were divided into fixed-size patches, which were transformed into sequential inputs via linear projection and position embedding, and then fed into a multi-layer Transformer Encoder. Each encoding layer consisted of multi-head self-attention, a feed-forward network, and layer normalization to capture global dependencies. Finally, the CLS token output was passed through a multi-layer perceptron (MLP) classification head to achieve a three-category prediction of disaster severity (mild, moderate, or severe).

For training, we built the ViT model using PyTorch and the timm library. We used the AdamW optimizer for parameter updates, with a learning rate of 1×10^{-4} , weight decay of 1×10^{-4} , and a batch size of 32. We used cross-entropy loss, and the maximum number of training epochs was 10. To ensure model robustness, we employed three-fold cross validation, stratifying the entire dataset according to its class distribution. In each fold iteration, the training set comprised approximately two-thirds of the dataset, and the validation set comprised approximately one-third. Out-of-fold (OOF) predictions were also saved for subsequent error analysis and confidence studies. Furthermore, we categorized misclassified samples into three types, namely overconfidence, ambiguity, and medium states, as defined in Section 3.2 (Disagreement-Driven Arbitration Framework). This categorization enables a more detailed diagnosis of failure patterns and reveals potential limitations of the ViT model in disaster assessment tasks.

Vision Transformer (ViT)

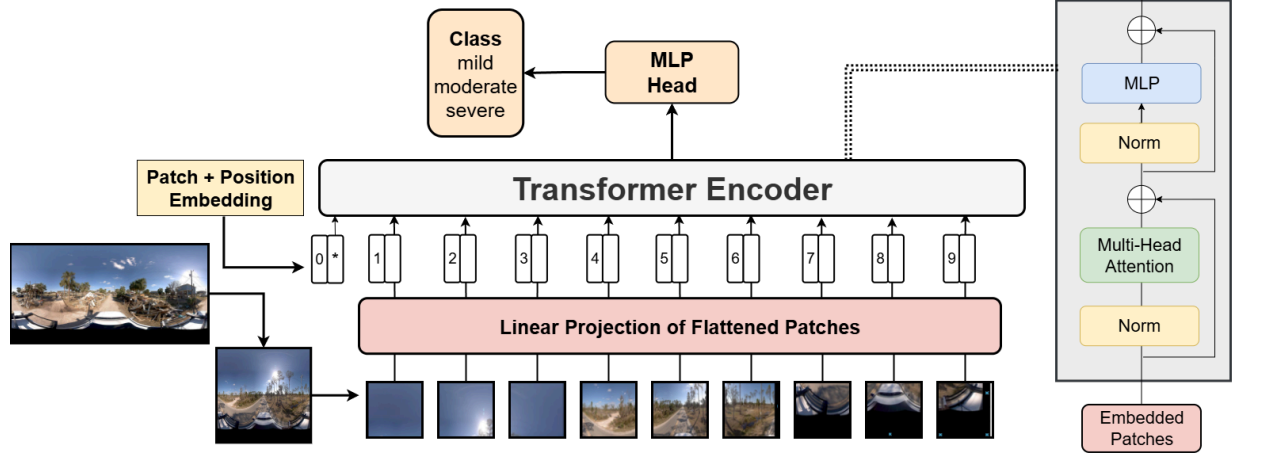


Figure 2. Vision Transformer (ViT) Framework for Disaster Assessment

3.1.2 CLIP-Text Encoder Architectures

In a text-only baseline experiment, we used CLIP’s text encoder as a standalone classifier to isolate and evaluate the contribution of the text modality to disaster damage assessment. Specifically, we set up two variants. The first, CLIP-Text Encoder (LLM captions), uses disaster descriptions automatically generated by GPT-4o-mini. These descriptions typically have broader and more abstract semantic representations, summarizing the overall characteristics of the disaster scene. They are used to test whether synthetic language can serve as an effective input modality for disaster severity classification. The second, CLIP-Text Encoder (Human captions), uses descriptions written by trained human annotators. These descriptions focus more on visible, fine-grained disaster signs, such as fallen trees, building debris, and damaged infrastructure, and more directly reflect specific disaster indicators than LLM-generated text.

In implementation, we used the CLIP text encoder (Transformer architecture, 12-layer encoder, 512-dimensional word embedding, maximum sequence length 77) to convert input text into a 512-dimensional semantic vector, which was then mapped to a three-category space (mild, moderate, and severe) via a linear layer. During training, all texts underwent a unified tokenization and encoding process. The classification head parameters were trained from scratch on the disaster dataset, while the CLIP text encoder was fine-tuned based on pre-trained weights. Both text models used three-fold stratified cross-validation with identical hyperparameter settings (learning rate 1×10^{-4} , batch size 32, and AdamW optimizer) to ensure comparability of results. By comparing LLM-based automatic descriptions with human-written objective descriptions, we were able to systematically analyze the differential role of different types of linguistic information in disaster assessment, further revealing the unique contributions and limitations of text modalities in disaster severity assessment.

3.1.3 Contrastive Language-Image Pre-training (CLIP) Architectures

To learn robust multimodal representations for disaster assessment, we employed a cross-modal contrastive learning framework based on the CLIP architecture. The core goal of this task is to align visual and textual modalities, establishing consistent representations in a shared semantic space that

effectively capture the severity of damage caused by disasters and their context. Compared to methods relying solely on visual models, this cross-modal approach offers enhanced interpretability and robustness, particularly in the face of scene complexity, class imbalance, and ambiguous visual cues. As shown in Figure 3, during training, each sample consists of a post-disaster street-view image and its corresponding text description. The text descriptions, which characterize the nature and severity of the damage, can be categorized into two sources: those written by human annotators, which offer high fidelity and fine-grained information; and those automatically generated by a large language model (LLM), specifically GPT-4o-mini in this study. By leveraging both human-generated and LLM-generated descriptions, we can systematically compare the impact of different text sources on model learning and explore the potential of LLMs in assisting disaster assessment.

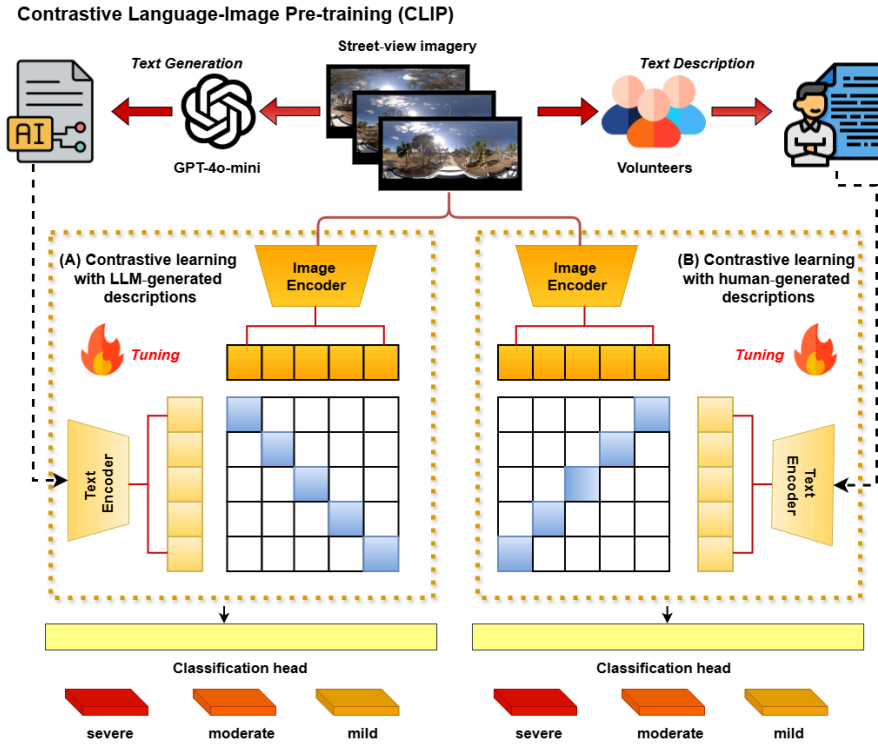


Figure 3. Contrastive Learning for Disaster Assessment with Human vs. LLM-Generated Descriptions.

Visual and textual features are extracted using a pre-trained CLIP model, where the image is processed through a visual encoder (ViT-B/16) and the text is processed through a transformer-based text encoder. The resulting embeddings are projected into a joint representation space where cross-modal alignment can be learned. During training, we optimize a single-directional InfoNCE loss, where each image serves as the query and its associated text description as the positive key. The objective encourages the model to increase the similarity between matched image–text pairs while minimizing the similarity between mismatched pairs in a batch. This is formulated as:

$$\mathcal{L}_{\text{contrast}} = -\frac{1}{N} \sum_{i=1}^N \log \frac{\exp(\text{sim}(x_i, y_i)/\tau)}{\sum_{j=1}^N \exp(\text{sim}(x_i, y_j)/\tau)} \quad (1)$$

Here, x_i and y_i denote the image and text embeddings of the i -th sample, $\text{sim}(x,y)$ represents cosine similarity between two normalized embeddings, and τ is a temperature scaling factor.

To further support downstream classification, we append a lightweight linear classification head to the combined embedding of the image and text modalities. This head is trained to predict one of three disaster severity levels (mild, moderate, or severe) using the standard cross-entropy loss:

$$\mathcal{L}_{\text{cls}} = - \sum_{i=1}^N \sum_{c=1}^C y_{ic} \log \hat{y}_{ic} \quad (1)$$

where $C=3$ denotes the number of severity classes, and \hat{y}_{ic} is the predicted softmax probability for class c of the i -th sample.

The final training objective combines the contrastive and classification losses as a weighted sum:

$$\mathcal{L}_{\text{total}} = \lambda \mathcal{L}_{\text{contrast}} + (1 - \lambda) \mathcal{L}_{\text{cls}} \quad (1)$$

with a tunable hyperparameter $\lambda \in [0,1]$ controlling the trade-off between representation alignment and classification accuracy. This hybrid training strategy enables the model to produce representations that are both semantically aligned across modalities and effective for downstream disaster assessment tasks such as damage severity prediction.

In summary, this cross-modal contrastive learning framework is expected to enhance the robustness and interpretability of disaster assessment models. It also provides a principled setting for evaluating the quality of text descriptions generated by humans and LLMs, as we expect LLMs to be able to autonomously generate text content in batches. Furthermore, this approach lays the foundation for subsequent analysis of model reliability and error characteristics.

Finally, we evaluate the full vision–language alignment capability of CLIP by jointly leveraging both image and text inputs. Two multimodal baselines are considered. CLIP (Image + LLM captions): Combines CLIP image embeddings with GPT-4o-mini–generated captions. This setting assesses whether automatically generated descriptions, despite being abstract and generalized, can provide complementary semantic cues when fused with visual features. CLIP (Image + Human captions): Combines CLIP image embeddings with human-written captions. Human text typically emphasizes fine-grained, object-level disaster indicators, and its integration with visual features allows us to examine whether precise linguistic cues can enhance classification performance. Both multimodal baselines use the same CLIP backbone to ensure comparability with the unimodal settings. By contrasting LLM-based and human-based captions, we highlight how different sources of textual information interact with vision features in disaster severity classification.

3.2 Disagreement-Driven Arbitration Framework

Considering that disaster assessment and decision-making in the disaster field place extremely high demands on model reliability and interpretability, we designed a confidence analysis method based on misclassified samples to deeply evaluate the performance of different models in disaster assessment tasks.

The core goal of this method is to distinguish two main sources of error: (1) overconfident errors caused by misleading significant but irrelevant features; and (2) ambiguous errors caused by multiple conflicting or insufficient evidence.

Specifically, we first extracted examples from the test set for all models (ViT-B/16, ViT-B/32, Text Encoder, CLIP, etc.) whose predictions were inconsistent with the true labels. This study employed a three-fold cross-validation and statistically analyzed all prediction errors across the entire dataset. These error examples formed the core focus of subsequent analysis. For each error example, we recorded the model's predicted probability distribution for the three disaster severity categories (mild, moderate, and severe), which reflects the model's confidence in each category. The overall workflow of this procedure is illustrated in Figure 4.

We defined the confidence margin of an error as the difference between the model's probability for the incorrectly predicted category and its probability for the true category. A high confidence score indicates that the model is extremely confident in the incorrect category, often implying that significant but irrelevant clues are misleading the model. This type of error is defined as an overconfidence error. A low confidence score indicates that the model's probabilities for different categories are close, reflecting conflicting or ambiguous features within the scenario, preventing the model from making a clear distinction. This type of error is defined as an ambiguity error. Based on this definition, we classify all erroneous samples into three categories. Overconfident: predicted probabilities are significantly higher than the true category; Medium: the difference between the predicted and true category probabilities is moderate, indicating a transitional state; and Ambiguous: the difference between the predicted and true category probabilities is extremely small, indicating that the model is trapped in uncertainty. This structured categorization of errors provides a foundation for systematically analyzing the reliability of model predictions and how different architectures handle uncertainty in disaster assessment tasks.

From the practical perspective of disaster assessment, overconfidence errors are particularly undesirable because they are difficult to detect and can mislead decision-making in disaster management, as false certainty can have serious consequences. In contrast, ambiguity errors, while reflecting model uncertainty, provide opportunities for human-machine collaboration. Experts can participate in assessing these uncertain situations and make informed judgments. Therefore, the ideal model does not eliminate all ambiguity, but rather one that minimizes overconfidence while transparently labeling uncertainty.

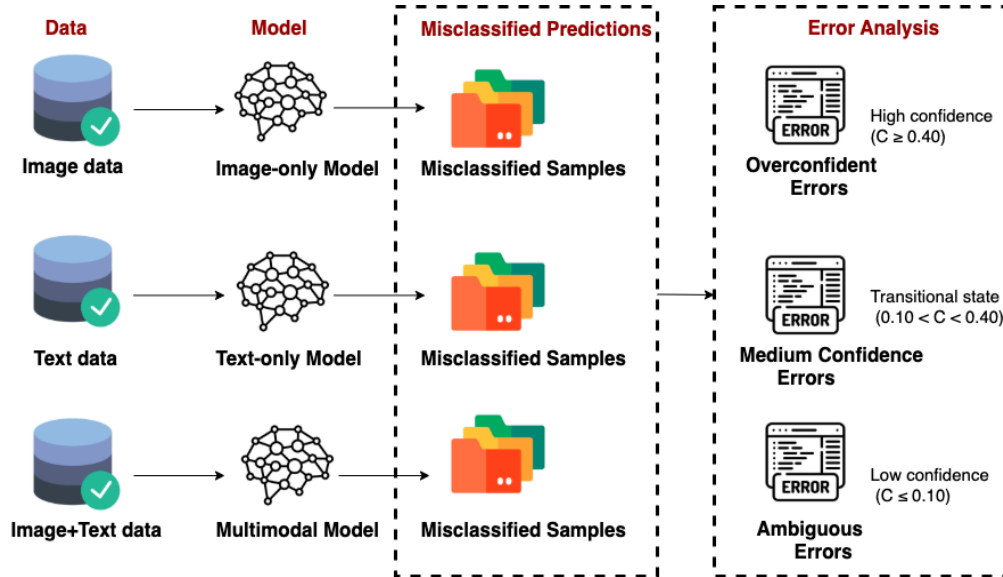


Figure 4. Framework of Confidence-Based Error Analysis in Disaster Assessment Models.

However, error analysis alone is insufficient to address model reliability issues in real-world deployments. To further improve performance while balancing accuracy and robustness, we propose a lightweight Disagreement-Driven Arbitration Framework. The core idea of this framework is that when two models agree on a prediction, the prediction is accepted. When there is a disagreement, a lightweight logistic regression meta-classifier is introduced to arbitrate and determine which prediction should be trusted. The meta-classifier's input includes not only the confidence scores and uncertainty metrics (entropy) from the models themselves, but also the disaster feature information extracted by semantic probes (such as fallen trees, building debris, damaged infrastructure, and flooded roads). The combination of these features, determined through ablation experiments, ultimately serves as the basis for arbitration.

This mechanism enables refined judgment on disagreement cases: when ViT is overconfident, the robustness of CLIP prevents misjudgments; and when CLIP is ambiguous, ViT's strong discriminative power provides clearer decisions. Ultimately, all prediction results are fed into the classification layer, which outputs three disaster severity categories (mild, moderate, and severe).

In summary, this framework effectively reduces the risk of overconfidence while ensuring high accuracy, significantly improving the model's usability and interpretability in disaster awareness tasks. Compared to a single model, the disagreement-driven arbitration approach better leverages the complementary strengths of multiple models, demonstrating significant potential for disaster decision-making and emergency management.

3.3 Semantic Detection

To support the disagreement-driven arbitration framework proposed in Section 3.2, this paper further constructs a set of semantic probe scores to characterize the response intensity of post-disaster street-view

images across different disaster semantic dimensions, and uses them as explicit input features for the arbitration classifier.

Based on street-view data characteristics of hurricane disasters and emergency management practices, this paper selects four representative disaster indicators as semantic probes: fallen trees, building debris, damaged infrastructure, and flooded roads. These indicators cover key dimensions such as the natural environment, built environment, infrastructure, and transportation systems, and can reflect the comprehensive impact of disasters on the socio-environmental system from a complementary perspective. It should be noted that this set of semantic probes is not fixed and can be expanded or adjusted according to specific disaster types.

As shown in Figure 5, during the semantic probe construction process, spaCy is first used to perform word segmentation and syntactic analysis on the text, extracting candidate phrases highly related to disaster semantics. A rule-based filtering and whitelist mechanism is used to retain domain-specific expressions and remove generalized or non-discriminative words. Then, based on predefined semantic dimension anchors, the log-odds ratio is used to discriminately score the candidate phrases and categorize them into the highest-scoring disaster semantic dimension. For each semantic dimension, the top-N phrases with the highest scores are selected, and diverse natural language semantic prompts are generated through template expansion, forming a corresponding semantic prompt set (prompts_XXX.json), which serves as the text input for the subsequent CLIP model.

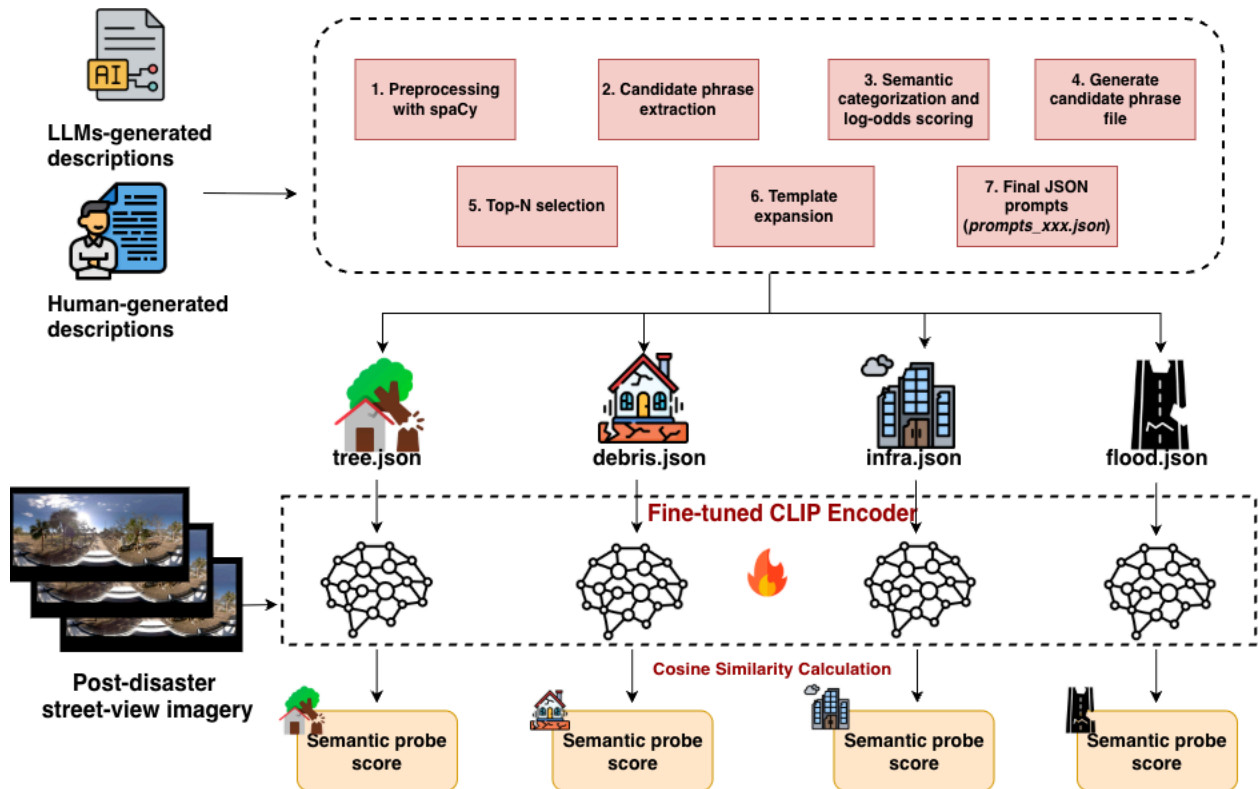


Figure 5. Workflow of Semantic Detection of Disaster Indicators Using Fine-tuned CLIP Encoder.

During the model inference phase, post-disaster street view images and the aforementioned semantic cues are input into the fine-tuned CLIP encoder. The CLIP model is fine-tuned with both manually annotated text and LLM-generated text as semantic inputs, used for joint embedding representations of images and text. The model measures the semantic alignment strength between the image and each disaster semantic cues by calculating the cosine similarity between the image embedding and the text embedding. To improve the stability of the score, the similarity results corresponding to multiple cues within the same semantic dimension are aggregated using pooling strategies (such as max pooling or mean pooling) to obtain a dimensional semantic probe score. Therefore, each post-disaster street-view image can be represented as a semantic probe vector consisting of four scalar values, corresponding to four disaster indicators: fallen trees, building debris, damaged infrastructure, and flooded roads. This semantic probe score, as one of the explicitly constructed discriminative features, is used as input along with the model confidence and uncertainty measure in Section 3.2 to train the divergence-driven arbitration classifier.

4. Experiments

4.1 Dataset and Preprocessing

In this study, we leveraged the Hurricane Damage Street-View Imagery dataset constructed by Yang et al. (2025). As shown in Figure 6, this dataset systematically documents the damage caused by 2024 Hurricane Milton in Horseshoe Beach in Florida along the Gulf Coast, providing unique high-resolution, geotagged, and temporally matched evidence for disaster damage assessment research. The dataset contains 2,556 post-disaster street view images. Each post-disaster image was manually classified into three damage severity levels: mild (658 images), moderate (1,196 images), and severe (702 images). The damage severity labels were manually assigned by multiple trained annotators according to predefined visual criteria, focusing on observable disaster impacts such as fallen trees, building debris, damaged infrastructure, and inundated roads. To ensure annotation consistency and accuracy, a cross-validation process was conducted among annotators before finalizing the labels.

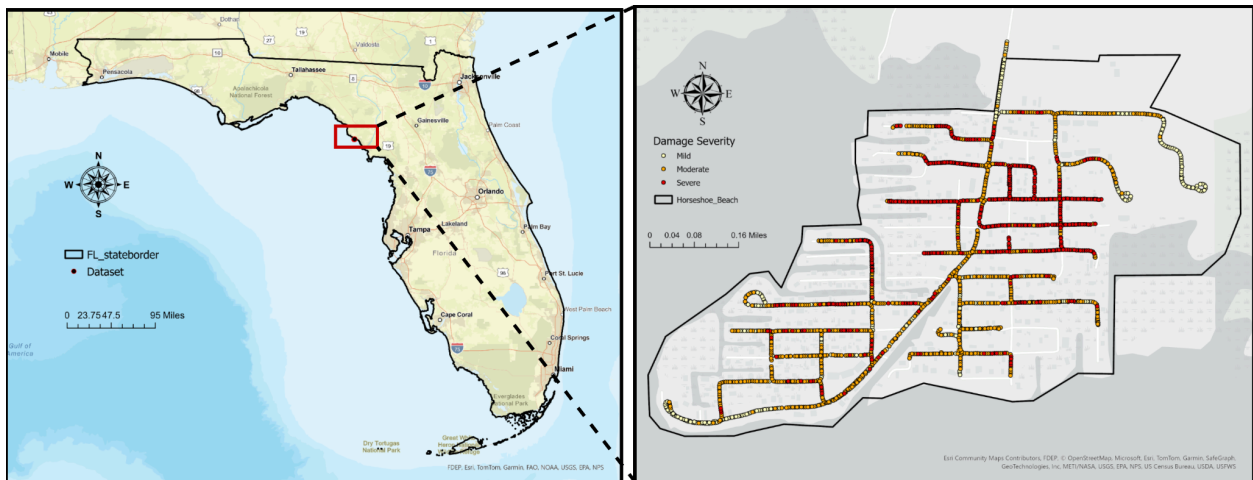


Figure 6. Hurricane Milton Damage Mapping and Street-View Sample Distribution

To enhance the interpretability and semantic depth of disaster assessment, we conducted a second round of fine-grained annotation using a dual-source strategy that integrates large language model

(LLM)-generated and human-labeled text descriptions. To facilitate automated annotation, we employed two cost-effective large language models, GPT-4o-mini and Gemini 2.0 Flash-Exp, which offer a favorable balance between annotation quality, inference speed, and computational cost for large-scale image labeling. Their generated captions were compared with the original street-view images using CLIPScore (Radford et al., 2021), and the higher-scoring outputs were selected as the textual dataset for CLIP input. We chose the result generated by GPT-4o-mini.

The automated annotation process was guided by a structured prompt designed to constrain the model's behavior and reduce hallucinations. Specifically, the model was instructed to act as a disaster damage annotator and to describe only damage evidence that was explicitly visible in each image. The prompt emphasized factual, image-grounded descriptions and prohibited speculative or inferred content. The model was required to generate a concise damage description of approximately 50 words, focusing on multiple observable damage dimensions, including fallen trees, damaged buildings, debris accumulation, and flooding conditions. All outputs were constrained to a predefined JSON schema to ensure structural consistency and facilitate downstream parsing.

In parallel, four trained volunteers independently provided manual annotations of post-disaster images, focusing on object-level cues such as debris on the road, fallen trees, and damaged houses. This single-temporal human annotation process was consistent with the fundamental task of the CLIP model, which aims to learn the alignment between post-disaster images and post-disaster textual semantics. Such annotations closely mirror the way human observers perceive and interpret disaster scenes.

As shown in Figure 7, each sample is accompanied by parallel text descriptions generated by both humans and the LLM, enabling a systematic comparison of automated and manual perception of the same visual scene. This dataset design ensures the robustness and scientific nature of classification experiments while providing rich support for semantically interpretable analysis. This provides a solid foundation for evaluating the role of textual information in improving disaster assessment models and promoting the practical application of human-machine collaboration.

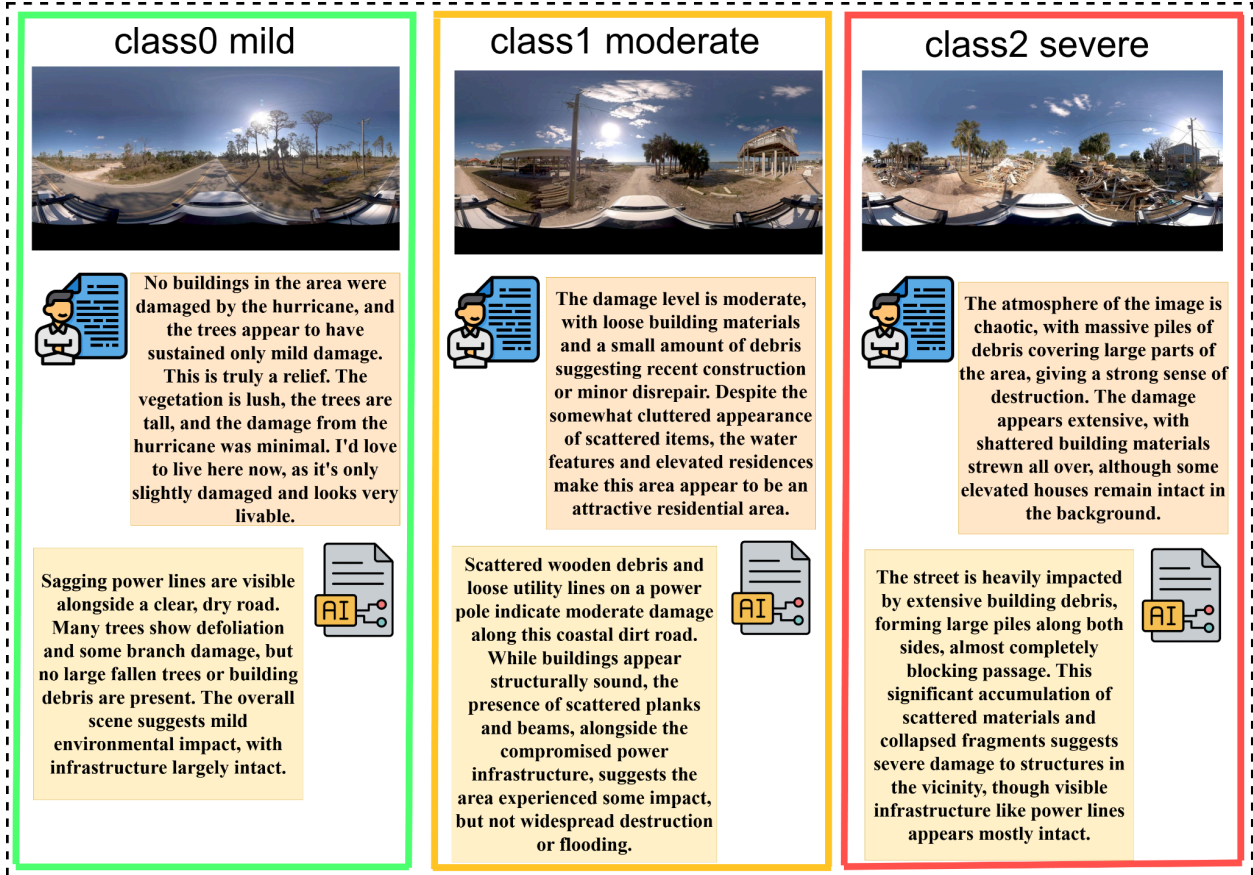


Figure 7. Examples of Disaster Severity Categories with Human- and LLM-Generated Descriptions

4.2 Implementation

All experiments were implemented in PyTorch using pre-trained models from the timm and CLIP libraries. To ensure fair comparison across unimodal and multimodal settings, all models were trained and evaluated under consistent data splits and hyperparameter configurations unless otherwise stated.

For image-based experiments, ViT-Base-Patch16-224 and ViT-Base-Patch32-224 were fine-tuned on post-disaster street-view images resized to 224×224 , with standard normalization and random horizontal flipping applied during training. Models were optimized using AdamW with a learning rate of 1×10^{-4} , weight decay of 1×10^{-4} , batch size 32, and a maximum of 10 epochs. Text-only baselines employed the CLIP text encoder, using either human-written descriptions or LLM-generated captions. A linear classification head was trained on top of the text embeddings for disaster severity prediction. Multimodal CLIP models jointly leveraged image and text embeddings and were trained using a contrastive learning objective combined with a classification loss, following the framework described in Section 3.1.3. All experiments adopted three-fold stratified cross-validation, and out-of-fold predictions were retained for subsequent confidence-based error analysis and arbitration.

4.3 Evaluation Metrics

To assess the semantic alignment between textual descriptions and their corresponding street-view images, we employed CLIPScore, a reference-free evaluation metric derived from a pre-trained Contrastive Language–Image Pretraining (CLIP) model (Radford et al., 2021). CLIPScore quantifies how well an image–text pair aligns within the shared multimodal embedding space learned during CLIP’s training.

For each image–text pair, the CLIP model encodes the image I and the corresponding caption T into their respective embeddings, $\mathbf{v}_I \in \mathbb{R}^d$ and $\mathbf{v}_T \in \mathbb{R}^d$, where d is the dimensionality of the shared multimodal embedding space. The CLIPScore is then defined as the cosine similarity between the two normalized embeddings:

$$\text{CLIPScore}(I, T) = \cos(\mathbf{v}_I, \mathbf{v}_T) = \frac{\mathbf{v}_I \cdot \mathbf{v}_T}{\|\mathbf{v}_I\| \|\mathbf{v}_T\|} \quad (1)$$

A higher CLIPScore indicates stronger semantic consistency between the image and its description. CLIPScore does not require ground-truth captions, making it especially useful in evaluating LLM-generated outputs in open-ended disaster contexts. In addition to CLIPScore, we evaluated classification performance using a comprehensive set of five standard metrics: Accuracy, Recall, Precision, Sample-Weighted F1-score (SW-F1), and Matthews Correlation Coefficient (MCC). These metrics are computed based on the confusion matrix components: true positives (TP), false positives (FP), true negatives (TN), and false negatives (FN), and are formally defined as follows:

$$\text{Accuracy} = \frac{TP + TN}{TP + TN + FP + FN} \quad (8)$$

$$\text{Recall} = \frac{TP}{TP + FN} \quad (9)$$

$$\text{Precision} = \frac{TP}{TP + FP} \quad (10)$$

$$\text{SW-F1} = 2 \times \frac{\text{Precision} \times \text{Recall}}{\text{Precision} + \text{Recall}} \quad (11)$$

$$\text{MCC} = \frac{TP \cdot TN - FP \cdot FN}{\sqrt{(TP + FP)(TP + FN)(TN + FP)(TN + FN)}} \quad (12)$$

5. Results

5.1 Comparative Evaluation of Models

Table 1 summarizes the classification performance of all baseline models across five key metrics along with CLIPScore for the multimodal variants. These results offer comparative insights into the effectiveness of image-only, text-only, and multimodal models for disaster severity classification.

Table 1. Comparative Evaluation of Image-only, Text-only, and Multimodal Models on Disaster Severity Classification.

Model	Modality	Accuracy	Recall	Precision	SW-F1	MCC	Clipscore
ViT-B/16	Image Only	0.7261	0.7261	0.7320	0.7240	0.5653	-
ViT-B/32	Image Only	0.7433	0.7433	0.7597	0.7386	0.5947	-
Text Encoder (LLM)	Text Only	0.6307	0.6307	0.6331	0.6261	0.4126	-
Text Encoder (Human)	Text Only	0.6710	0.6710	0.6779	0.6715	0.4788	-
CLIP (LLM)	Image+Text	0.7238	0.7238	0.7249	0.7229	0.5644	0.2467
CLIP (Human)	Image+Text	0.7422	0.7422	0.7504	0.7403	0.5915	0.2701
ViT-B/32 + CLIP(LLM)	Image+Text	0.8279	0.8065	0.8555	0.8261	0.7305	

Table 1 shows that image-based models perform well in post-disaster image classification, with ViT-B/32 outperforming ViT-B/16 (accuracy 0.7433 and 0.7261, respectively). This demonstrates that, despite using larger patches and resulting in coarser spatial details, ViT-B/32 offers advantages in computational efficiency and overall stability for this task.

On the text-based unimodal baseline, the CLIP text encoder performs worse than the image-based model overall. Specifically, manually written disaster descriptions (accuracy 0.6710) outperform the LLM-generated descriptions (accuracy 0.6307), demonstrating that the fine-grained, observable disaster feature information contained in human annotations is more effective for classification. When we describe an image, we also lose some information, so it is not surprising that the accuracy is lower than that of the image-based model.

In multimodal experiments, the CLIP model with combined image and text input showed improved overall performance compared to its unimodal counterpart. Specifically, CLIP-Human (accuracy 0.7422) using human descriptions outperformed CLIP-LLM (accuracy 0.7238) and also demonstrated higher semantic consistency in the Clipscore metric (0.2701 vs. 0.2467). While the CLIP model demonstrated satisfactory accuracy and was superior to text-based models, it was still lower than image-based models. While text can provide some supplementary semantic information, in the task of disaster severity, which relies heavily on visual evidence, imagery remains the primary driver, and the gains from text require more sophisticated modeling to fully realize them.

Finally, our proposed disagreement-driven arbitration framework achieved the best performance among all models, achieving an overall accuracy of 0.8279, significantly outperforming both unimodal and traditional multimodal baseline models. Improvements were achieved across the board in metrics such as

recall (0.8065), precision (0.8555), F1 score (0.8261), and MCC (0.7305). These results demonstrate that the arbitration framework effectively integrates the complementary strengths of ViT and CLIP, improving not only prediction performance but also the reliability and robustness of the model for disaster assessment tasks.

Figure 8 systematically illustrates the spatial distribution of disaster severity and the misclassification patterns of different models. The Ground Truth map (top left) shows that severe disasters (red dots) are highly concentrated along the core streets and southern corridors of the study area, while mild disasters (green dots) are more prevalent in the peripheral areas, exhibiting significant spatial heterogeneity. The Ground Truth map displays the disaster classification results for the entire study area. In the ViT-B/32 misclassification results (top right), the model captures the general pattern of disaster distribution well. However, within the central and southern areas with high concentrations of severe disasters, there are many instances of misclassifying severe disasters as moderate, indicating a lack of spatial sensitivity for high-severity disasters. Furthermore, in the peripheral areas with mild disasters, the model exhibits a tendency to overclassify, resulting in a decrease in local spatial consistency. In contrast, the CLIP-LLM misclassification results (bottom left) exhibit more dispersed spatial patterns, with errors occurring almost throughout the study area. In particular, the discriminatory nature of mild and moderate disasters exhibits high instability. This suggests that the text-generated input from the LLM does not provide sufficient spatial discrimination, resulting in a lack of clustering and spatial consistency in the results. The disagreement-driven arbitration framework (bottom right) significantly outperforms the single model in spatial performance, with fewer and more concentrated misclassification points, particularly in core streets and the southern severe disaster cluster. This framework more accurately maintains the spatial distribution of disaster severity, preventing underestimation of severe disasters. Furthermore, in the peripheral mild disaster areas, the framework effectively reduces large-scale excessive misclassifications, resulting in a spatial pattern closer to the true distribution. Overall, Figure 8 shows the spatial differences between different models in disaster severity identification. ViT provides strong global perception but is prone to confusion at a finer level. By observing the dispersion of misclassification points across the entire region and the high frequency of confusion between mild and moderate categories, we conclude that the CLIP-LLM lacks stable spatial discrimination. The disagreement-driven arbitration framework combines the strengths of both models, improving not only overall classification performance but also enhancing the reliability of the results and their coupling with the true disaster pattern in the spatial dimension.

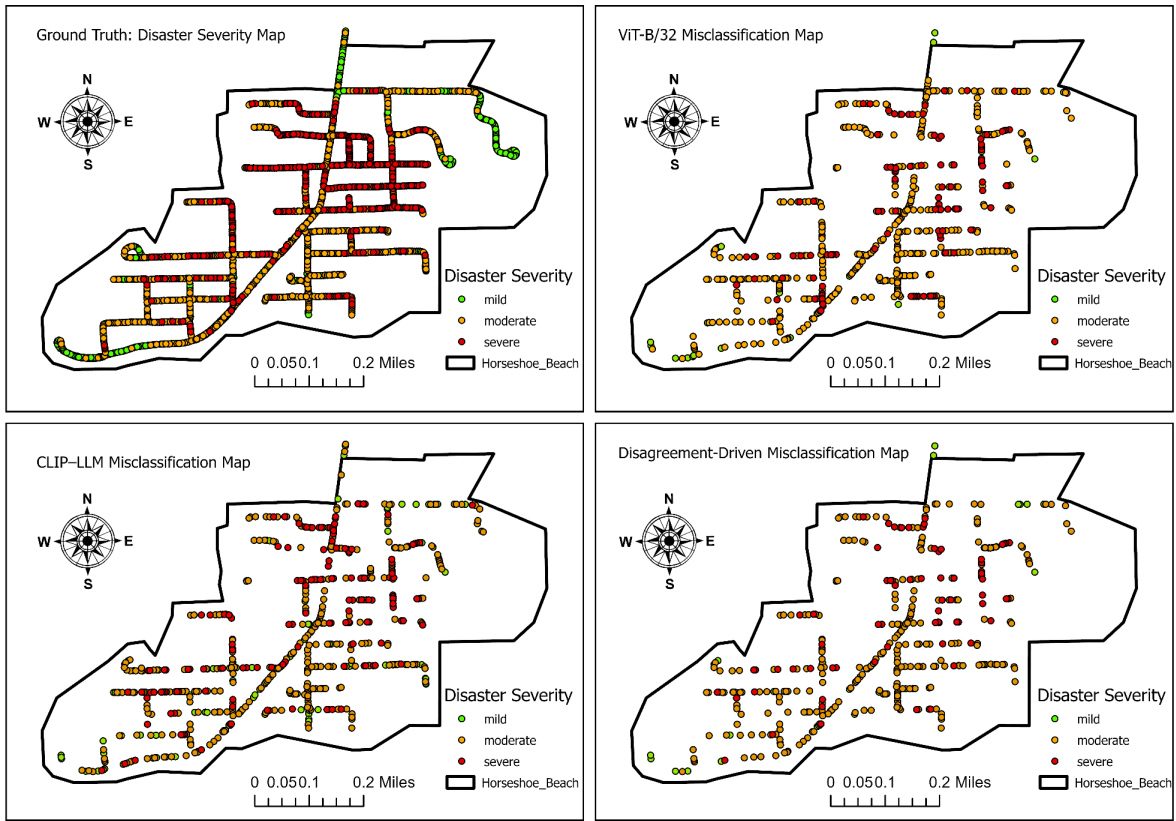


Figure 8. Comparison of Ground Truth and Model-Based Disaster Severity Maps.

5.2 Reliability Analysis of Misclassified Samples

Table 2 systematically analyzes the misclassification patterns of different models from the two dimensions of confidence level and disaster level, revealing the differences in model reliability in disaster assessment tasks.

Table 2. Confidence- and Severity-Based Misclassification Profiling of Image-, Text-, and Multimodal Models. Overconfident, Medium, and Ambiguous represent the misclassification distribution at different confidence levels; Mild Mis, Moderate Mis, and Severe Mis represent the misclassification proportions at different disaster levels.

Model	Modality	Overconfident	Medium	Ambiguous	Mild Mis	Moderate Mis	Severe Mis
ViT-B/16	Post Image	64.86%	27.14%	8.00%	40.43%	35.00%	24.57%
ViT-B/32	Post Image	70.58%	21.04%	8.38%	47.26%	27.90%	24.85%
Text Encoder (LLM)	Text Only	47.78%	37.71%	14.51%	38.14%	38.67%	23.20%
Text Encoder (Human)	Text Only	53.27%	33.65%	13.08%	30.20%	39.95%	29.85%
CLIP (LLM)	Image+Text	0.00%	55.18%	44.82%	39.73%	24.25%	21.91%
CLIP (Human)	Image+Text	0.00%	66.82%	33.18%	40.49%	19.06%	24.89%

In image-based unimodal models, both the ViT-B/16 and ViT-B/32 models exhibited high rates of overconfidence errors (64.86% and 70.58%, respectively). Their incorrect predictions were often accompanied by excessively high confidence levels, reflecting a serious lack of calibration. This pattern reflects the tendency of image-based models to make "pattern recognition" type decisions, drawing overly confident conclusions based on salient visual features. However, overconfidence errors are particularly dangerous in disaster scenarios, as they can lead to incorrect judgments in high-risk situations and thus mislead emergency response efforts.

In contrast, the error distribution characteristics of text-based unimodal models differ. The text encoder based on LLM-generated descriptions exhibited a higher rate of ambiguity errors (14.51%), indicating that the model tends to hesitate when faced with semantically conflicting or highly uncertain disaster scenarios, thus demonstrating semantic instability. The model based on human-generated text improved this problem somewhat, but its misclassification rate for severe disasters reached 29.85%. This suggests that while human-generated text enhances class separability, it still exhibits significant vulnerability in extreme disaster scenarios.

Among multimodal models, the CLIP framework demonstrated significant reliability advantages. Whether combining LLM-generated or human-generated text, the overconfidence error was 0%, highlighting the potential of cross-modal feature alignment in mitigating high-confidence errors. However, its error distribution varies across different text sources. CLIP (LLM)'s errors are primarily concentrated in the ambiguity interval (44.82%), indicating a tendency to be cautious in semantically

uncertain samples. CLIP (Human)'s errors, on the other hand, are more concentrated in the medium confidence interval (66.82%), and its misclassification rate is lowest at medium disaster levels (19.06%), demonstrating stronger ability to discern category boundaries. Notably, ambiguity errors can be mitigated by incorporating expert secondary assessments, further highlighting the CLIP model's advantages in disaster assessment.

In summary, reliability should take precedence over accuracy in disaster scenarios. Compared to unimodal approaches relying solely on images or text, the multimodal CLIP model excels in reducing overconfidence errors and enhancing model robustness, providing a more solid foundation for building trustworthy disaster management and decision support systems. Building on these findings, we further designed the disagreement-driven arbitration framework, which leverages the complementary strengths of ViT and CLIP to refine predictions on disagreement cases and deliver more reliable disaster assessment outcomes.

5.3 Semantic Detection

After constructing the semantic probes, we aggregated candidate phrases across four dimensions (flood, trees, building debris, and infrastructure) and visualized them using a word cloud to visually illustrate the distribution of disaster semantic cues. As shown in Figure 9, the results reveal several high-frequency and representative disaster indicator phrases, such as "flooding drainage issue," "downed power lines," "fallen tree," and "debris pile." These terms capture typical post-disaster physical damage patterns, encompassing scenarios ranging from flooded roads and fallen trees to power outages and building debris. Overall, the word cloud not only reveals the most frequently captured core semantic elements in disaster text descriptions but also highlights the complementary relationships between the various dimensions: flood cues emphasize environmental processes (e.g., "flooding issue"), trees and debris highlight visually significant physical damage, and infrastructure phrases reveal functional damage (e.g., "downed power lines" and "collapsed bridge"). These results demonstrate that the constructed semantic probes systematically cover multiple aspects of disaster impacts, providing a solid semantic foundation for subsequent CLIP semantic profile analysis. Moreover, the semantic detection system we built can be used for subsequent similar hurricane disasters, and the methodology can also be extended to other types of disasters.

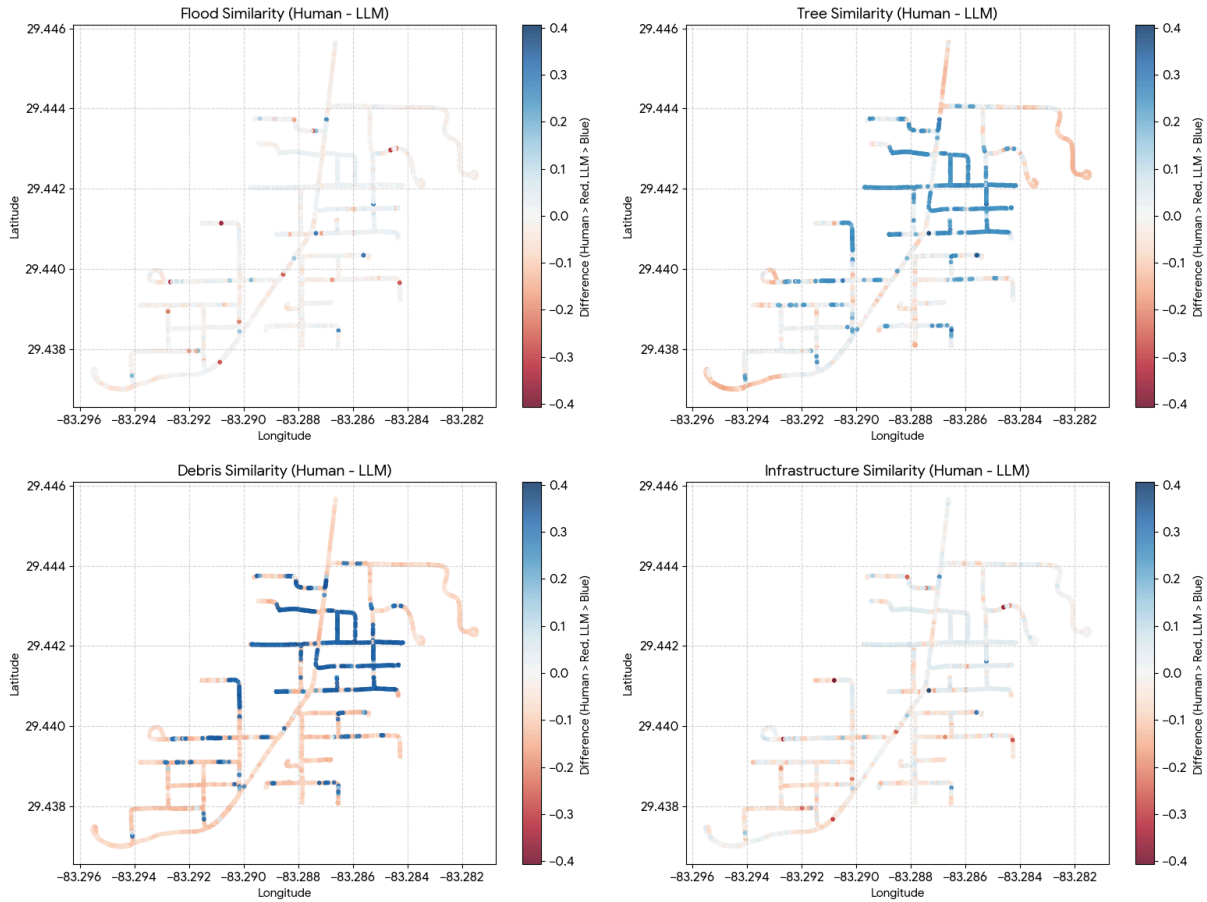


Figure 10. Mapping Semantic Divergence: Human vs. LLM Similarity Scores

Based on the above analysis, this study further provides two trained and validated CLIP models (CLIP-Human and CLIP-LLM) and constructs a standardized disaster semantic probe text system. This system covers key disaster types such as floods, trees, debris, and infrastructure, and can serve as the semantic input interface for the model in post-disaster scenarios. In future applications, users only need to upload post-disaster images, and the system can call the pre-trained model and semantic probes to automatically calculate the similarity distribution between the image and disaster semantics, thereby quickly generating interpretable damage heatmaps. This mechanism effectively realizes a closed-loop transformation from "semantic understanding" to "disaster detection," enabling the model to complete post-disaster information extraction and spatial damage identification without human intervention, providing real-time support for emergency response. This process not only demonstrates the transferability and universality of semantic probes but also provides a new language-driven detection paradigm for the field of disaster geography, enabling interpretive analysis results to be directly transformed into practically valuable automated disaster assessment tools.

5.4 Ablation Study

To systematically evaluate the role of different features in a disagreement-driven arbitration framework, this study designed ablation experiments. The initial configuration of the arbitrator incorporates three types of features: confidence, uncertainty, and semantic probes (including four dimensions: trees, debris, infrastructure, and flooding). These serve as inputs to a logistic regression arbitrator. The ablation experiments gradually remove or combine these features to examine their relative contributions to the arbitration process. Specifically, we first use only confidence as input to test its independent effect; then we add an uncertainty metric to confidence to assess its marginal gain; and further, we combine semantic probe information to examine whether semantic features provide complementary value. As a control, we also test a configuration that relies solely on semantic probes to verify their independent discriminative power. With this design, ablation experiments can reveal the mechanisms by which different features function in the arbitration framework, providing empirical evidence for optimizing the final arbitration strategy.

As shown in Table 3, ablation experiment results clearly demonstrate the impact of different feature combinations on arbitration performance. First, relying solely on confidence (LOGREG_conf) achieves the highest performance (Accuracy = 0.976, Macro-F1 = 0.965), demonstrating that confidence is the most discriminative feature in arbitration. Second, introducing uncertainty (LOGREG_conf+unc) or further combining it with semantic probes (LOGREG_conf+unc+probe) on top of confidence leads to a decrease in model performance, indicating that these features are somewhat redundant with confidence in the current task scenario and fail to provide additional benefits. Finally, using semantic probes alone (LOGREG_probe_only) significantly underperforms other configurations (Accuracy = 0.607, Macro-F1 = 0.560), confirming that semantic features are insufficient to independently support arbitration discrimination and are more suitable as auxiliary information. Overall, the logistic regression arbitrator achieves optimal performance on divergent samples by relying primarily on confidence. This finding provides a basis for the subsequent design of transparent arbitration rules.

Table 3. Ablation study of logistic regression arbitration with different feature configurations.

Arbitration Setting	Features Used	Accuracy	Macro-F1
LOGREG_conf [$\tau=0.35$]	Confidence only	0.976	0.965
LOGREG_conf+unc [$\tau=0.40$]	Confidence + Uncertainty	0.940	0.932
LOGREG_conf+unc+p robe [$\tau=0.45$]	Confidence + Uncertainty + Semantic Probes	0.940	0.932
LOGREG_probe_only [$\tau=0.50$]	Probes only	0.607	0.560

Based on ablation experiments, we summarize a transparent and explainable arbitration rule. When ViT's confidence is significantly higher than CLIP and the predicted distribution is stable, ViT's results should

be given priority. In this case, ViT's strong discriminative ability can provide more accurate identification of disaster severity. When ViT shows overconfidence or disagrees in high-uncertainty scenarios, CLIP's results should be given priority. At this time, CLIP's robustness and cross-modal feature alignment capabilities can effectively avoid misleading predictions. This rule is not only verified in the experimental results, but also meets the actual demand for reliability priority in disaster scenarios. ViT provides high-resolution discrimination, while CLIP provides more robust protection. The combination of the two ensures more reliable decisions on divergent samples.

6. Discussions

This study focuses on post-disaster assessment, proposing and validating a multimodal framework based on disagreement-driven arbitration. Comparing different models, we found that, while image-based models (such as ViT) have strong discriminative power in capturing disaster severity, they are prone to overconfidence errors. On the other hand, multimodal models (such as CLIP) demonstrate greater robustness and interpretability, effectively reducing the risk of misjudgment, particularly in high-uncertainty scenarios. By combining the complementary strengths of these two approaches, the proposed arbitration mechanism improves both reliability and interpretability, providing a new approach for rapid and reliable decision-making in disaster scenarios.

However, this study also has limitations. First, the experiments focused on a single disaster case (such as a hurricane) and a limited geographic scope, and the model's generalization across regions and disaster types requires further testing. Second, the limited gains from semantic probes and uncertainty features in the arbitration process suggest the need for future research on more efficient semantic modeling methods and more robust uncertainty estimation mechanisms. Finally, while we have proposed confidence-driven arbitration rules, dynamically adjusting them to varying disaster levels remains a worthy research direction.

As shown in Figure 11, we propose two promising directions for future research. **Pseudo Post-Disaster Image Synthesis:** Based on a generative model, this method generates pseudo post-disaster imagery from pre-disaster street scenes and text descriptions. This method then enhances training and evaluation by comparing it with real post-disaster imagery. This not only helps alleviate the shortage of real post-disaster data but also supports pre-disaster rehearsals and risk simulations. **Zero-Shot Object Detection and Segmentation:** Leveraging a vision-language model (such as Gemini-2.5), this method automatically detects and semantically segmented disaster-related objects without the need for additional annotation, significantly reducing manual annotation costs and improving the model's flexibility and transferability to disaster response.

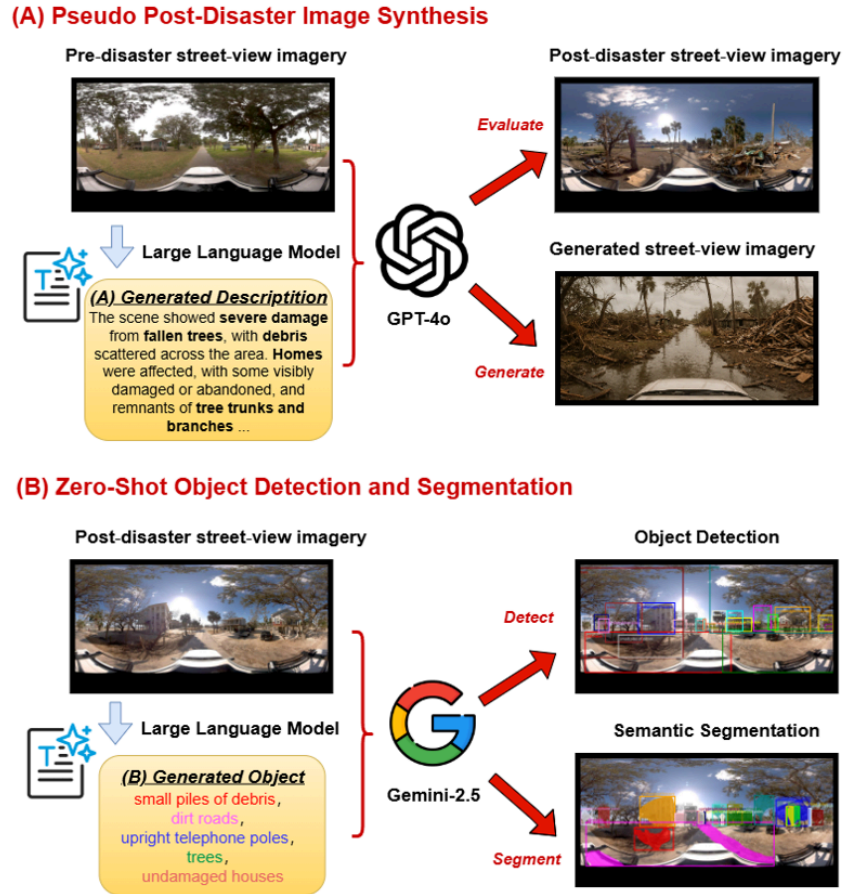


Figure 11. Future directions: (A) pseudo post-disaster image synthesis and (B) zero-shot object detection and segmentation.

7. Conclusion

This study addresses the limited reliability and interpretability of models in post-disaster assessment by proposing a disagreement-driven arbitration framework. We systematically compare the performance of unimodal image, unimodal text, multimodal CLIP, and arbitration models in disaster severity classification. Results show that the image model (ViT) exhibits strong discriminative power but is prone to overconfidence errors; the text model can provide some supplementary semantic information but suffers from limited stability; and the multimodal CLIP model exhibits advantages in robustness, particularly in high-uncertainty scenarios. Our proposed disagreement-driven arbitration framework effectively integrates the complementary properties of ViT and CLIP, significantly improving classification reliability and spatial consistency while boosting the overall accuracy to 82.79%, the best and most competitive result to date for disaster severity assessment based on street-view imagery.

Furthermore, through confidence analysis and semantic probe construction, we further explore the sources of model errors from misclassified samples, revealing the distinct risk characteristics of overconfidence and semantic ambiguity in disaster tasks, and propose corresponding improvements for human-machine collaboration. This research not only enriches the modeling methodology for disaster assessment but also

provides a reference for model selection and credible interpretation in emergency decision-making. In summary, this study demonstrates the effectiveness and practicality of the disagreement-driven arbitration framework in disaster assessment tasks, providing methodological support for building more reliable, interpretable disaster intelligence systems.

Acknowledgements

We would like to acknowledge the funding agencies for sponsoring this investigation. This article is based on work supported by two grants. One is from the U.S. National Science Foundation - Collaborative Research: HNDS-I: Cyberinfrastructure for Human Dynamics and Resilience Research (Award No. 2318206). The other grant is from the Gulf Research Program under the U.S. National Academies of Sciences, Engineering, and Medicine (SCON-10000653). Any opinions, findings, conclusions, or recommendations expressed in this material are those of the authors and do not necessarily reflect the views of the funding agencies.

Disclosure statement

No potential conflict of interest was reported by the authors.

References

- Agathokleous, E., Saitanis, C. J., Fang, C., & Yu, Z. (2023). Use of ChatGPT: What does it mean for biology and environmental science? *Science of The Total Environment*, 888, 164154. <https://doi.org/10.1016/j.scitotenv.2023.164154>
- Alvarez Leon, L. F., & Quinn, S. (2019). The value of crowdsourced street-level imagery: Examining the shifting property regimes of OpenStreetCam and Mapillary. *GeoJournal*, 84(2), 395–414. <https://doi.org/10.1007/s10708-018-9865-4>
- Ding, N., Qin, Y., Yang, G., Wei, F., Yang, Z., Su, Y., Hu, S., Chen, Y., Chan, C.-M., Chen, W., Yi, J., Zhao, W., Wang, X., Liu, Z., Zheng, H.-T., Chen, J., Liu, Y., Tang, J., Li, J., & Sun, M. (2023). Parameter-efficient fine-tuning of large-scale pre-trained language models. *Nature Machine Intelligence*, 5(3), 220–235. <https://doi.org/10.1038/s42256-023-00626-4>
- Feng, J., Tan, H., Li, W., & Xie, M. (2022). Conv2NeXt: Reconsidering Conv NeXt Network Design for Image Recognition. 2022 International Conference on Computers and Artificial Intelligence Technologies (CAIT), 53–60. <https://doi.org/10.1109/CAIT56099.2022.10072172>
- Gao, G., Ye, X., Li, S., Huang, X., Ning, H., Retchless, D., & Li, Z. (2024). Exploring flood mitigation governance by estimating first-floor elevation via deep learning and google street view in coastal Texas. *Environment and planning B: Urban analytics and city science*, 51(2), 296-313.
- Gimpel, H., Hall, K., Decker, S., Eymann, T., Lämmermann, L., Mädche, A., Röglinger, M., Ruiner, C., Schoch, M., Schoop, M., Urbach, N., & Vandrik, S. (2023). Unlocking the power of generative AI models and systems such as GPT-4 and ChatGPT for higher education: A guide for students and lecturers (Working Paper Nos. 02–2023). Hohenheim Discussion Papers in Business, Economics and Social Sciences. <https://www.econstor.eu/handle/10419/270970>

Gupta, N. (2021). A Pre-Trained Vs Fine-Tuning Methodology in Transfer Learning. *Journal of Physics: Conference Series*, 1947(1), 012028. <https://doi.org/10.1088/1742-6596/1947/1/012028>

Haas, L., Alberti, S., & Skreta, M. (2023). Learning Generalized Zero-Shot Learners for Open-Domain Image Geolocalization (No. arXiv:2302.00275). arXiv. <https://doi.org/10.48550/arXiv.2302.00275>

Jayati, S., Choi, E., Burton, H., & Newsam, S. (2024). Leveraging Large Multimodal Models to Augment Image-Based Building Damage Assessment. *Proceedings of the 7th ACM SIGSPATIAL International Workshop on AI for Geographic Knowledge Discovery*, 79–85. <https://doi.org/10.1145/3687123.3698291>

Lozano, C., & Tien, D. (2023). *Street-view imagery for post-disaster assessment: A review of advances and challenges*. *International Journal of Disaster Risk Reduction*, 95, 103841. <https://doi.org/10.1016/j.ijdr.2023.103841>

Li, H., Deuser, F., Yina, W., Luo, X., Walther, P., Mai, G., Huang, W., & Werner, M. (2024). Cross-View Geolocalization and Disaster Mapping with Street-View and VHR Satellite Imagery: A Case Study of Hurricane IAN (No. arXiv:2408.06761). arXiv. <https://doi.org/10.48550/arXiv.2408.06761>

Li, L., Ye, Y., Jiang, B., & Zeng, W. (2024, June 6). GeoReasoner: Geo-localization with Reasoning in Street Views using a Large Vision-Language Model. *Forty-first International Conference on Machine Learning*. <https://openreview.net/forum?id=WWo9G5zyh0>

Li, S., Liu, Q., Pan, Z., & Wu, X. (2025). CLIP-BCA-Gated: A Dynamic Multimodal Framework for Real-Time Humanitarian Crisis Classification with Bi-Cross-Attention and Adaptive Gating. *Applied Sciences*, 15(15), 8758. <https://doi.org/10.3390/app15158758>

Liu, Y., Ding, J., Deng, G., Li, Y., Zhang, T., Sun, W., Zheng, Y., Ge, J., & Liu, Y. (2024). Image-Based Geolocation Using Large Vision-Language Models (No. arXiv:2408.09474). arXiv. <https://doi.org/10.48550/arXiv.2408.09474>

Liu, Z., Hu, H., Lin, Y., Yao, Z., Xie, Z., Wei, Y., Ning, J., Cao, Y., Zhang, Z., Dong, L., Wei, F., & Guo, B. (2022). Swin Transformer V2: Scaling Up Capacity and Resolution. 12009–12019. https://openaccess.thecvf.com/content/CVPR2022/html/Liu_Swin_Transformer_V2_Scaling_Up_Capacity_and_Resolution_CVPR_2022_paper.html

Liu, Z., Lin, Y., Cao, Y., Hu, H., Wei, Y., Zhang, Z., Lin, S., & Guo, B. (2021). Swin Transformer: Hierarchical Vision Transformer Using Shifted Windows. 10012–10022. https://openaccess.thecvf.com/content/ICCV2021/html/Liu_Swin_Transformer_Hierarchical_Vision_Transformer_Using_Shifted_Windows_ICCV_2021_paper

Ma, Z., Li, L., Li, J., Hua, W., Liu, J., Feng, Q., & Miura, Y. (2025). A Multimodal, Multilingual, and Multidimensional Pipeline for Fine-grained Crowdsourcing Earthquake Damage Evaluation. arXiv preprint arXiv:2506.03360. <https://doi.org/10.48550/arXiv.2506.03360>

Mahabir, R., Schuchard, R., Crooks, A., Croitoru, A., & Stefanidis, A. (2020). Crowdsourcing Street View Imagery: A Comparison of Mapillary and OpenStreetCam. *ISPRS International Journal of Geo-Information*, 9(6), Article 6. <https://doi.org/10.3390/ijgi9060341>

- OpenAI, Achiam, J., Adler, S., Agarwal, S., Ahmad, L., Akkaya, I., Aleman, F. L., Almeida, D., Altenschmidt, J., Altman, S., Anadkat, S., Avila, R., Babuschkin, I., Balaji, S., Balcom, V., Baltescu, P., Bao, H., Bavarian, M., Belgum, J., ... Zoph, B. (2024). GPT-4 Technical Report (No. arXiv:2303.08774). arXiv. <https://doi.org/10.48550/arXiv.2303.08774>
- Radford, A., Kim, J. W., Hallacy, C., Ramesh, A., Goh, G., Agarwal, S., Sastry, G., Askell, A., Mishkin, P., Clark, J., Krueger, G., & Sutskever, I. (2021). Learning Transferable Visual Models From Natural Language Supervision (No. arXiv:2103.00020). arXiv. <https://doi.org/10.48550/arXiv.2103.00020>
- Sánchez, I. A. V., & Labib, S. M. (2024). Accessing eye-level greenness visibility from open-source street view images: A methodological development and implementation in multi-city and multi-country contexts. *Sustainable Cities and Society*, 103, 105262. <https://doi.org/10.1016/j.scs.2024.105262>
- Selvaraju, R. R., Cogswell, M., Das, A., Vedantam, R., Parikh, D., & Batra, D. (2017). Grad-cam: Visual explanations from deep networks via gradient-based localization. In *Proceedings of the IEEE international conference on computer vision* (pp. 618-626).
- Wang, C., Antos, S. E., Gosling-Goldsmith, J. G., Triveno, L. M., Zhu, C., von Meding, J., & Ye, X. (2024). Assessing Climate Disaster Vulnerability in Peru and Colombia Using Street View Imagery: A Pilot Study. *Buildings*, 14(1), Article 1. <https://doi.org/10.3390/buildings14010014>
- Wang, S., Hu, T., Xiao, H., Li, Y., Zhang, C., Ning, H., Zhu, R., Li, Z., & Ye, X. (2024). GPT, large language models (LLMs) and generative artificial intelligence (GAI) models in geospatial science: a systematic review. *International Journal of Digital Earth*, 17(1), 2353122.
- Wang, Z., Xu, D., Khan, R. M. S., Lin, Y., Fan, Z., & Zhu, X. (2024). LLMGeo: Benchmarking Large Language Models on Image Geolocation In-the-wild (No. arXiv:2405.20363). arXiv. <https://doi.org/10.48550/arXiv.2405.20363>
- Wightman, R. (2019). Pytorch image models (timm).
- Woo, S., Debnath, S., Hu, R., Chen, X., Liu, Z., Kweon, I. S., & Xie, S. (2023). ConvNeXt V2: Co-Designing and Scaling ConvNets With Masked Autoencoders. 16133–16142. https://openaccess.thecvf.com/content/CVPR2023/html/Woo_ConvNeXt_V2_Co-Designing_and_Scaling_ConvNets_With_Masked_Autoencoders_CVPR_2023_paper.html
- Wu, D., & Cui, Y. (2018). Disaster early warning and damage assessment analysis using social media data and geo-location information. *Decision Support Systems*, 111, 48–59. <https://doi.org/10.1016/j.dss.2018.04.005>
- Wu, Q., Xu, Y., Xiao, T., Xiao, Y., Li, Y., Wang, T., Zhang, Y., Zhong, S., Zhang, Y., Lu, W., & Yang, Y. (2024). Surveying Attitudinal Alignment Between Large Language Models Vs. Humans Towards 17 Sustainable Development Goals (No. arXiv:2404.13885). arXiv. <https://doi.org/10.48550/arXiv.2404.13885>
- Xin, Y., Luo, S., Zhou, H., Du, J., Liu, X., Fan, Y., Li, Q., & Du, Y. (2024). Parameter-Efficient Fine-Tuning for Pre-Trained Vision Models: A Survey (No. arXiv:2402.02242). arXiv. <https://doi.org/10.48550/arXiv.2402.02242>

- Xu, L., Zhao, S., Lin, Q., Chen, L., Luo, Q., Wu, S., Ye, X., Feng, H., & Du, Z. (2025). Evaluating large language models on geospatial tasks: a multiple geospatial task benchmarking study. *International Journal of Digital Earth*, 18(1), 2480268.
- Xue, Z., Zhang, X., Prevatt, D. O., Bridge, J., Xu, S., & Zhao, X. (2024). Post-hurricane building damage assessment using street-view imagery and structured data: A multi-modal deep learning approach (No. arXiv:2404.07399). arXiv. <https://doi.org/10.48550/arXiv.2404.07399>
- Ye, X., Li, S., Gao, G., Retchless, D., Cai, Z., Newman, G., ... & Duffield, N. (2024). 3D visualization of hurricane storm surge impact on urban infrastructure. *Urban Informatics*, 3(1), 9.
- Yamazaki, F., & Matsuoka, M. (2007). *Remote sensing technologies for post-earthquake damage assessment: A case study in Kobe City, Japan*. *Earthquake Spectra*, 23(1), 155–167. <https://doi.org/10.1193/1.2432323>
- Yang, Y., Wang, S., Li, D., Sun, S., & Wu, Q. (2024). GeoLocator: A Location-Integrated Large Multimodal Model (LMM) for Inferring Geo-Privacy. *Applied Sciences*, 14(16), Article 16. <https://doi.org/10.3390/app14167091>
- Yang, Y., Zou, L., Zhou, B., Li, D., Lin, B., Abedin, J., & Yang, M. (2025). Hyperlocal disaster damage assessment using bi-temporal street-view imagery and pre-trained vision models. *Computers, Environment and Urban Systems*, 121, 102335.
- Yang, Y., & Zou, L. (2025). Perceiving Multidimensional Disaster Damages from Street-View Images Using Visual-Language Models. *Abstracts of the ICA*, 10, 310.
- Zhai, W., & Peng, Z. R. (2020). Damage assessment using Google Street View: Evidence from Hurricane Michael in Mexico Beach, Florida. *Applied Geography*, 123, 102252. <https://doi.org/10.1016/j.apgeog.2020.102252>
- Zhao, X., Lu, Y., & Lin, G. (2024). An integrated deep learning approach for assessing the visual qualities of built environments utilizing street view images. *Engineering Applications of Artificial Intelligence*, 130, 107805. <https://doi.org/10.1016/j.engappai.2023.107805>